

See discussions, stats, and author profiles for this publication at: <https://www.researchgate.net/publication/227641225>

# Dynamic interfacial properties between a flexible-chain polymer and a thermotropic liquid crystalline polymer investigated by an ellipsoidal drop retraction method

ARTICLE in JOURNAL OF APPLIED POLYMER SCIENCE · NOVEMBER 2004

Impact Factor: 1.77 · DOI: 10.1002/app.21039

---

CITATIONS

9

---

READS

20

4 AUTHORS, INCLUDING:



Wei Yu

Shanghai Jiao Tong University

125 PUBLICATIONS 1,915 CITATIONS

SEE PROFILE

# Dynamic Interfacial Properties Between a Flexible-Chain Polymer and a Thermotropic Liquid Crystalline Polymer Investigated by an Ellipsoidal Drop Retraction Method

Ruobing Yu,<sup>1</sup> Wei Yu,<sup>1</sup> Chixing Zhou,<sup>1</sup> J. J. Feng<sup>2</sup>

<sup>1</sup>Department of Polymer Science and Engineering, Shanghai Jiao Tong University, Shanghai 200240, China

<sup>2</sup>The Levich Institute for Physicochemical Hydrodynamics, City College of the City University of New York, New York, New York 10031

Received 9 October 2003; accepted 11 May 2004

DOI 10.1002/app.21039

Published online in Wiley InterScience (www.interscience.wiley.com).

**ABSTRACT:** In this study, the dynamic interfacial properties between an isotropic polymer and a thermotropic liquid crystalline polymer (TLCP) were investigated by measuring the time-dependent interfacial tension between them. As a TLCP drop retracts in a flexible polymer matrix, the evolution of its shape is recorded by microscopy. By fitting the ellipsoidal model of Maffettone and Minale, the model of Marrucci and Santo, and large deformation ellipsoidal models by Jackson–Tucker and Yu–Bousmina, the interfacial tension could then be determined. It was found that the retrac-

tion of a TLCP ellipsoidal drop in a flexible polymer cannot be described by these models as accurately as in Newtonian systems. The apparent interfacial tension obtained from these models evolves with time; the evolution is ascribed to the slow relaxation of domain orientation within the TLCP drop. © 2004 Wiley Periodicals, Inc. *J Appl Polym Sci* 94: 1404–1410, 2004

**Key words:** thermotropic liquid crystalline polymer (TLCP); interfaces; relaxation; orientation; matrix

## INTRODUCTION

The physical properties of immiscible polymer blends are largely determined by the morphology of the phase domains generated during the blending process. Factors governing the development of the morphology of polymer blends include the composition, rheological properties of the components, processing conditions, and the interfacial properties. In the past decades, many efforts have been made to understand the factors governing the morphology of Newtonian systems.<sup>1–3</sup> However, our knowledge of blend systems consisting of rheologically complex fluids, such as polymeric fluids or anisotropic thermotropic liquid crystalline polymers (TLCPs),<sup>4</sup> is still very limited. Experiments<sup>5</sup> and numerical simulations<sup>6</sup> show that the relaxation of macromolecules substantially influences the evolution of the phase morphology. Nematic orientation of a liquid crystalline polymer (LCP) also affects the interfacial properties between the LCP and a flexible polymer.<sup>7</sup>

Although we have learned much about the mechanism of the deformation and relaxation of macromolecules, it is not straightforward to relate these mechanisms to the interfacial evolution. Furthermore, it is not clear how the interfacial properties (e.g., the interfacial tension) are influenced by the deformation and relaxation of macromolecules. Such influence is even more complex in LCP systems because of the orientation and orientation distribution of LCP molecules. Most investigations concerning TLCP-containing blends have focused on the relations between the morphology and the mechanical properties of the blend. Far less attention has been given to the interfacial tension between a TLCP and a flexible isotropic polymer. This is partly ascribed to experimental difficulties involved in the accurate measurement of the interfacial tension. Besides, a conceptual issue arises in dynamic situations. One can imagine that the interfacial tension between a TLCP and a flexible polymer might not be a constant when the macromolecules were not completely relaxed. Measuring the interfacial tension during the relaxation process of the macromolecules will probably reveal some interdependence between the macroscopic interfacial properties and the microscopic molecular dynamics. The aim of this work was to explore such coupling between two length scales during the retraction of a TLCP drop.

Measurements of the interfacial tension between polymers can be divided into static and dynamic methods.<sup>8</sup> Static methods (e.g., pendant drop, sessile

Correspondence to: C. Zhou (cxzhou@sjtu.edu.cn).

Contract grant sponsor: National Natural Science Foundation of China; contract grant numbers: 20174024, 20204007, and 50290090.

Contract grant sponsor: U.S. National Science Foundation; contract grant numbers: CTS-9984402 and CTS-0229298.

drop, and spinning drop) are based on the equilibrium shape of a droplet in a force field. These methods require accurate measurement of the density difference between the polymers. Also, a lengthy waiting time is needed to reach the equilibrium state because of the high viscosity of polymers, which incurs the risk of thermal degradation. Moreover, the interfacial tension measured by static methods is an equilibrium value, which may not represent the interfacial property between two components with complex microstructure during flow. Dynamic methods follow the change in the shape of a thread or an elongated droplet to an equilibrium shape. These include the method of thread breakup by Rayleigh instability, the retraction of an elongated droplet or a short fiber,<sup>9</sup> and the dynamic shear rheometry on emulsions.<sup>10</sup> The drop retraction method can be traced back to the pioneering work of Taylor,<sup>11</sup> who put forward a small-deformation theory in a viscous simple shear or extensional flow. In experimental measurement, the initial deformed drop was produced either by melting a short fiber<sup>12,13</sup> or by performing a preshear on a spherical drop.<sup>14,15</sup>

The same methods were also applied to the polymer/TLCPs. For example, the interfacial tension of TLCP (Vectra A900)/flexible polymers has been measured by both the thread-breakup method and the fiber-retraction method,<sup>16</sup> and TLCP (PSHQ6,12)/PDMS (poldimethylsiloxane) by thread breakup.<sup>17</sup> The interfacial tension between TLCP (Vectra B950) and FEP (fluorinated ethylene-propylene), TLCP (Vectra A 900), and PET [poly(ethylene terephthalate)] have been estimated from the harmonic-mean equation.<sup>4,18</sup> We found, however, that during the breakup of a long TLCP fiber immersed in a flexible polymer matrix, the interfacial instability does not appear as regular sinusoidal waves as on a flexible polymer fiber immersed in another flexible polymer. Therefore, it is impossible to calculate the interfacial tension directly from the Tomotika theory<sup>19</sup> with irregular waves. Here, we adopt the ellipsoidal drop retraction method to determine the interfacial tension, which has not been used before for flexible polymer/TLCP systems. To generate an ellipsoidal TLCP drop, we conducted experiments through the breakup of a long TLCP fiber and the retraction of a short fiber. The experiments showed that, after the breakup of a long TLCP fiber, the drops have long tails and do not retract as an ellipsoidal drop. It seems very difficult to describe such kinds of drops with long tails by available theories. We observed that the process of the retraction of a short fiber was divided into two stages: a short fiber shrinkage with constant cylindrical shape and formation of an ellipsoid from the shrunken fiber followed by retracting into a sphere. Therefore, the second stage in the retraction of short fiber will be used to determine the interfacial tension.

It should be pointed out that the interfacial tension determined by these methods is an "apparent" and "average" one, given that it is the macroscopic representation of the interfacial free energy changes with area in the interfacial layer. Therefore, all factors that can change the interfacial free energy will change the interfacial tension. "Average" means the interfacial tension is the mean value over the interfacial layer. Such an average approach is more significant on the interface between anisotropic and isotropic materials because the interfacial diffused layer is characterized by a more complicated structure and such an apparent interfacial tension is hard to determine experimentally.

There are several ellipsoidal models, such as the model of Maffettone and Minale,<sup>20</sup> the ellipsoidal model of Marrucci and Santo,<sup>21</sup> and the large-deformation ellipsoidal models of Jackson-Tucker<sup>22</sup> and Yu-Bousmina,<sup>23</sup> to calculate the interfacial tension. However, all these models are derived for Newtonian systems. Direct applications of these models to a TLCP/flexible chain polymer system will cause some problems because the viscoelasticity and complex polydomain structures in TLCP are not included in these models. Because the interfacial tension could be changed with the relaxation process of the internal structures in TLCP, we apply these models to a short period of TLCP drop retraction, and assume that the variation of texture structures or the relaxations of macromolecules are very small in such periods. The interfacial tension thus obtained is a function of retraction time, which is referred to as apparent dynamic interfacial tension or dynamic interfacial tension. The evolution of the dynamic interfacial tension reflects the variation of interfacial free energy, which depends on the viscoelasticity and mesoscopic structure of the components.

## RETRACTION MODELS

### Maffettone-Minale (MM) model

In the Maffettone-Minale model,<sup>20</sup> the drop shape is described by a symmetric, positive-definite, second-rank tensors  $S$  whose eigenvalues represent the square semiaxis of the ellipsoid. The evolution of  $S$  results from the competing actions of the interfacial tension and the drag exerted by the motion, and is first obtained by Maffettone and Minale<sup>20</sup> and applied in the measurement of the interfacial tension by Mo et al.<sup>25</sup> During the drop retraction, the major and minor semiaxes of the ellipsoid,  $L$  and  $B$ , satisfy

$$L^2 - B^2 = (L^2 - B^2)_{t=0} \times \exp \left[ -\frac{\sigma}{\eta_m R_0} \frac{40(p+1)}{(2p+3)(19p+16)} t \right] \quad (1)$$

where  $\sigma$  is the interfacial tension,  $\eta_m$  is the viscosity of matrix,  $R_0$  is the radius of the final sphere drop, and  $p$

is the ratio between the viscosity of the TLCP and the matrix. Hereafter, we will call  $L^2 - B^2$  the "shape parameter." Equation (1) is applicable to the retraction process of a Newtonian drop embedded in another Newtonian matrix, and the deformation of the drop should not be too large. From the measured evolution of  $L$  and  $B$ , the interfacial tension can be extracted from the slope of the plot  $\ln(L^2 - B^2)/(L^2 - B^2)_{t=0} \sim t$ .

### Marrucci and Santo (MS) model

Marrucci and Santo<sup>21</sup> developed a simple model for the time evolution of a drop subjected to an elongational flow. It is assumed that, for sufficiently small deformation rates, the droplet deforms to an ellipsoidal shape. In the absence of flow, the retraction process of the drop can be written as

$$\frac{d\rho}{dt} = \frac{1}{\tau_{MS}} \frac{\rho\{[(1 + 2/5p)/p]\rho\}^{1/8}(1 - \rho)}{1 + 2/5(p - 1)\rho^2} \quad (2)$$

where  $\rho = B/L$ . The characteristic time  $\tau_{MS}$  for the retraction is given in this case by

$$\tau_{MS} = \frac{\eta_m R_0}{0.465\sigma} \quad (3)$$

The model assumes affine deformation  $B = W$  because the original model is developed only for drop deformation in elongational flow. The way to extract the interfacial tension from eq. (2) is as follows. If  $\rho_t$  is the experimental value of the axis ratio measured at time  $t$ , then eq. (2) can be integrated to give

$$I(\rho_t) = \int_{\rho_t=0}^{\rho_t} \frac{1}{\rho} \frac{1 + 2/5(p - 1)\rho^2}{\{[(1 + 2/5p)/p]\rho\}^{1/8}(1 - \rho)} d\rho = \frac{t}{\tau_{MS}} \quad (4)$$

For each value of the measured axis ratio ( $\rho_t$ ), the integral can be computed. Then the interfacial tension can be determined from the slope of the plot  $I(\rho_t) \sim t$ .

### Large-deformation model

The ellipsoidal model of Maffettone and Minale can be applied only to small deformation of drops. If the deformation of the drop is large, other models, such as the Jackson–Tucker (JT) model<sup>22</sup> and the Yu–Bousmina (YB) model,<sup>23</sup> should be used to accurately capture the shape of the drop. In these models, the ellipsoidal drop is presented by a second-rank tensor  $\mathbf{G}$ .<sup>22,23,26</sup>  $\mathbf{G}$  is the inverse of the tensor  $\mathbf{S}$ . In the principal coordinates of the drop,  $\mathbf{G}$  can be expressed as

$$\mathbf{G} = \begin{pmatrix} 1/L^2 & 0 & 0 \\ 0 & 1/B^2 & 0 \\ 0 & 0 & 1/W^2 \end{pmatrix} \quad (5)$$

The evolution of  $\mathbf{G}$  is written as<sup>26</sup>

$$\frac{D\mathbf{G}_{ij}}{Dt} + L_{ki}\mathbf{G}_{kj} + \mathbf{G}_{ik}L_{kj} = 0 \quad (6)$$

where  $D/Dt$  is the material derivate and  $L_{ij}$  is the velocity gradient on the drop interface.  $L_{ij}$  has only diagonal components during retraction of the drop. Equation (6) can be reduced for the retraction process of a drop<sup>24</sup> [ $L(t)$  is major semiaxis of the ellipsoid], as follows:

$$\frac{d \ln L(t)}{dt} = L_{11}(t) \quad (7)$$

Similar expressions can be obtained for  $B$  and  $W$ . The interfacial tension can be extracted from eq. (7) if we can relate the velocity gradient  $L_{11}$  to the surface tension. The rationale for making such a connection is that the retraction of drop is driven by the interfacial tension. We can express the velocity gradient as a function of the characteristic time  $\tau$  by

$$L_{ij} = F'_{ij}(t)/\tau \quad \tau = \eta_m R/\sigma \quad (8)$$

where  $F_{ij}(t)$  are functions of the viscosity ratio and the shape of the drop. Two different approximate expressions for  $F'_{ij}$  have been derived. Yu and Bousmina<sup>23</sup> split the interfacial velocity gradient into a flow-dominated term and a term controlled by the interfacial tension. Jackson and Tucker<sup>22</sup> calculated  $L$  as an interpolation between the Eshelby model and a slender-body model. Using either the JT or YB model, eq. (7) can be integrated to give

$$\ln \frac{L(t)}{L_{t=0}} = \frac{1}{\tau} \int_0^t F'_{11}(t')/dt' = \frac{F_{11}(t)}{\tau} \quad (9)$$

The interfacial tension can then be determined from the slope of the plot  $\ln L(t)/L_{t=0} \sim F_{11}(t)$ . In principle, equations for  $B$  and  $W$  similar to eq. (9) can also be used to determine the interfacial tension.

## EXPERIMENTAL

### Materials

The materials used in this work were LC-5000 (Unichika, Inoue, Japan) and polycarbonate (Bayer PC2858; Bayer AG, Leverkusen, Germany). LC-5000 exhibits a crystalline-to-nematic melt transition point at 275°C, as measured with DSC from the first heat scan at a heating rate 20°C/min (Fig. 1). Above 275°C, LC-5000 is in the nematic phase. The glass-transition temperature of PC2858 is 150°C.

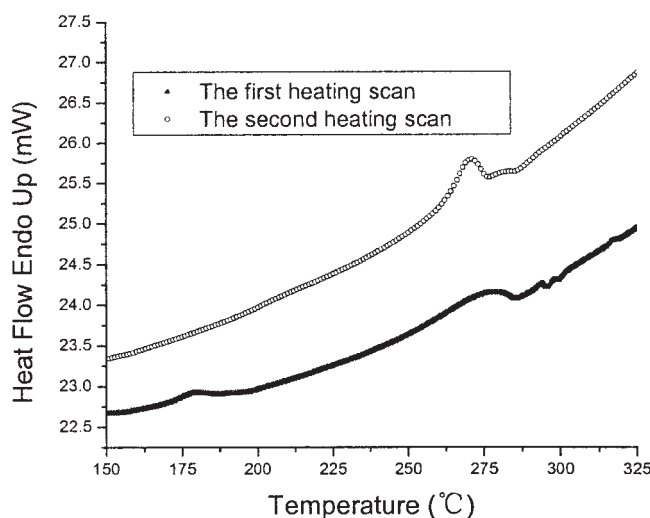


Figure 1 DSC of LC-5000.

### Rheological measurements

All rheological measurements were performed on a Haake RheoStress 300 rheometer (Haake, Bersdorff, Germany) at 295°C. Dynamic frequency sweep tests were used to determine the linear viscoelasticity of both materials. The geometry used for dynamic frequency sweep was parallel plate, with the diameter 20 mm and a gap 1 mm. Creep tests were used to determine the zero shear viscosity and creep compliance of LC-5000. Parallel-plate geometry (diameter 35 mm; gap  $\sim 1$  mm) was used in the creep tests.

### Interfacial tension measurement

As-received pellets of LC-5000 were dried at 180°C under nitrogen for 4 h and kept under vacuum at 90°C before further use. The matrix polymer, PC2858, was dried and kept at 90°C under vacuum for at least 3 days before use.

First, threads of LC-5000 were spun from a molten granule on a hot plate (295°C). Then the threads were cut into short fibers that were sandwiched between two PC (bisphenol-A polycarbonate) matrix plates. The sandwich was molded into thick films with a thickness of 0.6 mm at 240°C. During molding of the film, we increased the pressure gradually to ensure that any air bubbles trapped around the TLCP fibers had time to escape. Then the film was cut into 8  $\times$  8-mm squares containing one short fiber as a desired specimen.

Observations were carried out on an optical microscope (Leica, Wetzlar, Germany) with a camera and a hot stage at magnification of either  $\times 100$  or  $\times 40$ , depending on the drop size. The prepared specimen was put on the hot stage of the optical microscope and heated at 20°C/min to 240°C. The sample was maintained under this temperature for 5 min to allow the

matrix polymer, PC, to relax completely. Subsequently, the specimen was heated further at 40°C/min to the desired temperature of 295°C. The ensuing retraction of the short fiber was imaged and recorded. In most of our experiment systems, short fibers retracted to spheres, as shown in Figure 3. The images were analyzed using the image-analysis software Mivnt (Shanghai Optical Instrument Factory).

## RESULTS AND DISCUSSIONS

### Zero-shear viscosity

The zero-shear viscosity of PC2858 was determined by fitting the complex viscosity to the Ellis model and applying the Cox–Merz rule,  $\eta_0$  (PC2858) = 431.5 Pa s<sup>-1</sup>. Because LC-5000 does not show a plateau in the complex viscosity curve, it is difficult to determine its zero shear from dynamic experiments. Therefore, creep tests under a small constant stress were performed to obtain the viscosity under a lower shear rate. Figure 2 shows the creep curve of LC-5000 at 295°C, and the shear viscosity was calculated by the slope of the straight line. The shear viscosity of LC-5000 is 115.1 Pa.s. The viscosity ratio between LC-5000 and PC2858 is 0.267.

### Apparent interfacial tension

The retracting process of a short TLCP fiber in PC matrix is illustrated by the photographs in Figure 3. The fiber retracts into an ellipsoidal shape shortly after melting. The shape of the drop remains ellipsoidal during the whole process, which takes about 5–6 min. The two axes,  $L$  and  $B$ , can be readily measured from the photos because the longest axis of the drop is assumed to be parallel to the horizontal plane and no

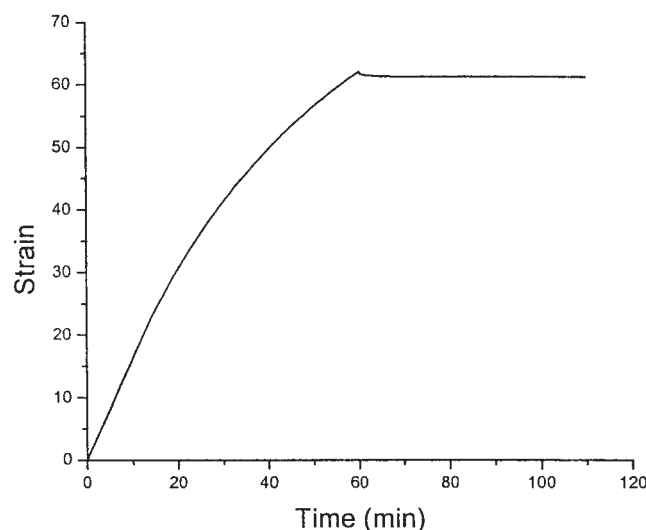
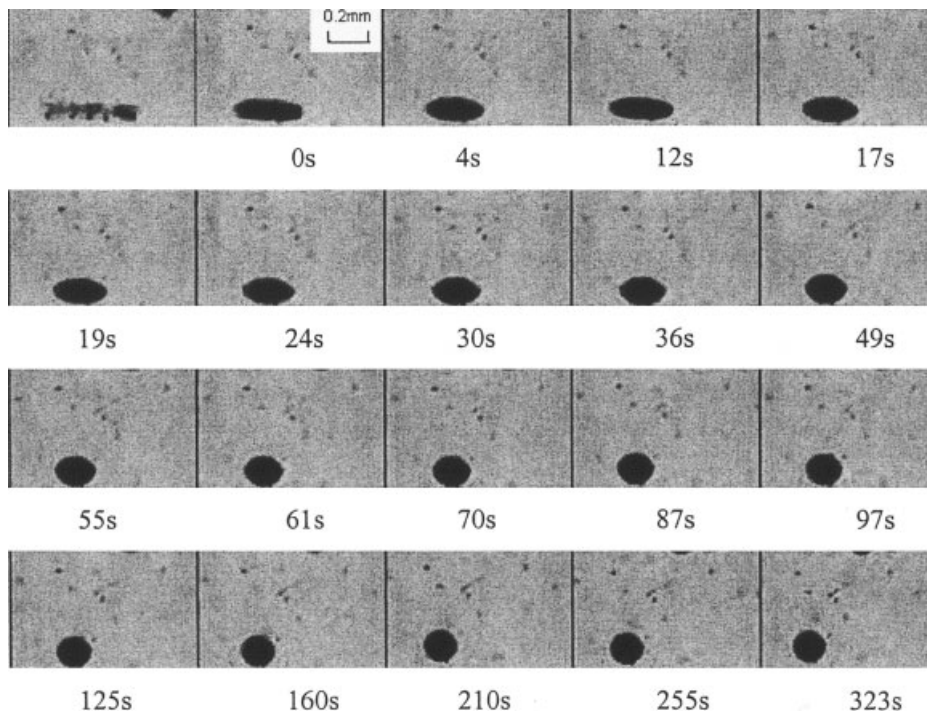


Figure 2 Creep curve and recovery of LC-5000 at 295°C (applied stress is 1 Pa).





**Figure 3** Retraction of short LC-5000 fiber in PC2858 matrix at 295°C.

rotation takes place during the retraction. The length of the third axis is calculated from conservation of the drop volume by  $R_0^3 = LBW$ , where  $R_0$  is the radius of the final sphere drop, which is 0.0795 mm in this case. The evolution of three semiaxes of the drop is shown in Figure 4. It should be noted that  $B$  and  $W$  are not equal until the very late stage of retraction, which means that the drop retains a nonaxisymmetric form during the early stage of retraction. Note also that the shape of the drop is not ellipsoidal until lasting 19 s after the start of the retraction. Therefore, the estimation of the third semiaxis of the drop from the volume

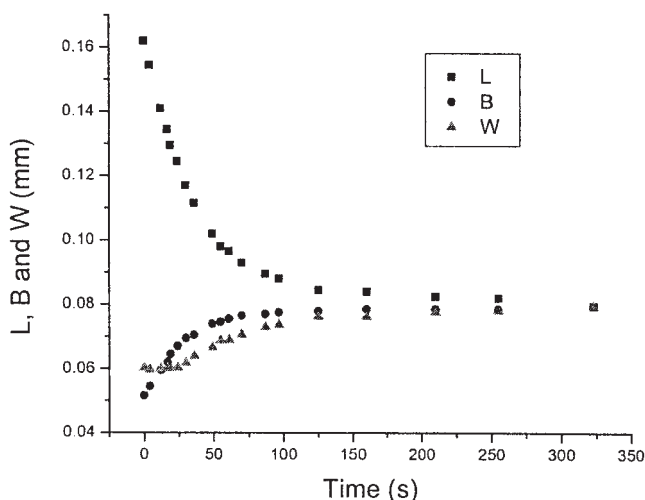


**Figure 4** Time evolution of three semiaxes for LC-5000 ellipsoidal drop in PC2858 matrix.

preservation of ellipsoid will suffer certain errors in the initial stage of retraction. We start the calculation of an apparent interfacial tension from ellipsoidal models (MM model; MS model; YB model and JT model) at about 19 s.

From the evolution of the three semiaxes, the apparent interfacial tension can be easily calculated from the MM model; the MS model; and the JT and YB models. As stated above, all these models are obtained from Newtonian systems. However, these models can be used in a short period such that the viscosity and elasticity of the components scarcely change. The interfacial tension thus obtained is an apparent one because it represents just an average effect of anisotropic interface between TLCP and the flexible-chain polymer. The apparent interfacial tension then is a function of time. The results are shown in Figure 5. All the results show a decrease of the apparent interfacial tension with the increase of time. Results of the MM, YB, and JT models have a similar pattern: a plateau appears at the beginning followed by a sharp decrease and again a slow decrease toward an equilibrium value. The main differences among results of the four models lie in the beginning of the retracting process. The MS model does not predict the plateau as the other models do because it is based on the assumption of affine deformation, which is not true in this case. The MM model is derived only for slightly deformed drops, and previous studies have shown that its use for large drop deformation may produce an apparent evolution of the interfacial tension in a Newtonian system with constant interfacial tension.<sup>24</sup> In our case,

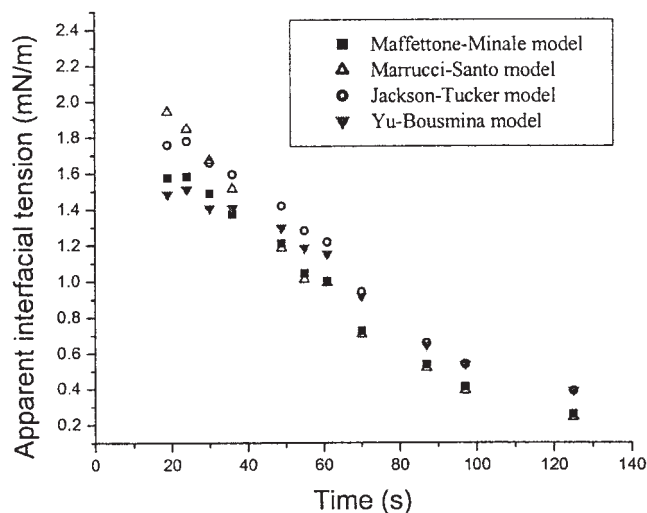


**Figure 5** Time evolution of the apparent interfacial tension between LC-5000 ellipsoid drop and PC2858 matrix.

however, the results of the MM model are close to the results given by large-deformation models (JT model and YB model) and MS model for later times. It is not clear why the small-deformation requirement appears to be less restrictive for the TLCP drop in our case than for the Newtonian drops previously studied. The apparent interfacial tension thus obtained is about 1.5–2.0 mN/m in the beginning of drop retraction and 0.3–0.4 mN/m as the equilibrium value. These values are much smaller than the interfacial tension, about 4–6 mN/m, between Vectra A900 and polyethersulfone.<sup>16</sup> Such a discrepancy is ascribed to the differences in the chemical structure and molecular weight of the polymers, and the macromolecular conformation of the liquid crystalline polymer.

From the preceding results, we can conclude that the apparent interfacial tension between a TLCP and a flexible polymer decreases with time, which is significantly different from that between two polymers with flexible chains. We believe that the evolution of the apparent interfacial tension is attributed to the relaxation processes in both phases. To substantiate this idea, we calculated the relaxation spectrum for LC-5000 and PC2858 to quantify the characteristic relaxation processes in these polymers. The relaxation spectrum of PC2858 is calculated from the dynamic modulus at 295°C using the nonlinear Tikhonov regularization method.<sup>27</sup> The relaxation spectrum of LC-5000 is calculated from a combined dynamic modulus, which is composed of the modulus from dynamic experiments and a calculated modulus from the creep tests. For the latter, the retardation spectrum of LC-5000 is calculated first from the creep compliance. Then a dynamic compliance is calculated from the retardation spectrum, which is further converted to the dynamic modulus. The combined dynamic moduli are shown in Figure 6. The weighted relaxation spec-

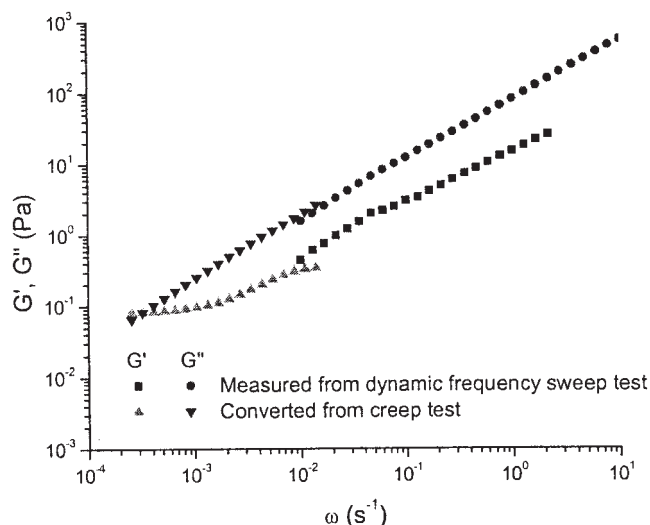


**Figure 6** Combined dynamic modulus of LC-5000 at 295°C.

trum of LC-5000, calculated from the combined dynamic modulus, and that of PC2858 are shown in Figure 7 [the peak of  $\lambda^*H(\lambda)$  is the characteristic relaxation time].

The relaxation time for PC is remarkably short, and it is believed to be fully relaxed before TLCP drop retraction. Consequently, the effect of viscoelasticity of PC on the apparent interfacial tension can be ignored, and only the relaxation of LC-5000 will influence the drop retraction. The nonequilibrium state of the TLCP molecules or microdomains is introduced during sample preparation and loading (e.g., spinning of the TLCP fiber and molding). The distorted orientational state and the accumulated stress will tend to relax during the experiment. This, we contend, gives rise to

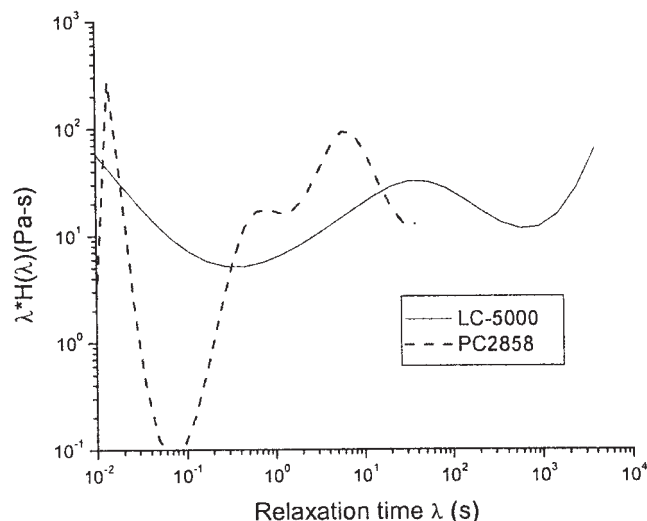


**Figure 7** Weighted relaxation spectrum of LC-5000 and PC2858 at 295°C.

the temporal evolution of the apparent interfacial tension.

From the weighted relaxation spectrum of LC-5000, we can find a peak with a relaxation time of about 50 s and an increase of  $\lambda^*H(\lambda)$  with  $\lambda$  at  $\lambda > 10^3$  s. The latter trend suggests a long relaxation time of LC-5000 at  $\lambda > 10^3$  s. An accurate determination of such a long relaxation time needs at least  $10^4$  s for the creep test, which is well beyond the time of our creep tests, 2400 s. Moreover, the storage modulus exhibits a plateau at low frequency, which is a characteristic solid-like behavior. Colby et al.<sup>28</sup> observed the same trend, arguing that a network of defect lines essentially makes the material a viscoelastic solid with a yield stress. Thus, we may conclude that there are two characteristic relaxation times for LC-5000,  $\lambda_1 \approx 50$  s and  $\lambda_2 > 10^3$  s. The long relaxation time  $\lambda_2$  is related to the relaxation of TLCP textures and defects. Its large value represents the well-known fact that defects and textures do not anneal out in stationary LCP samples for a long time, and perhaps never.<sup>28</sup> We may call this a textural time, or defect time, and it is believed to have little effect on the time evolution of the interfacial tension in our experiment. This is because the TLCP drop has completely retracted before the relaxation process, which corresponds to the occurrence of  $\lambda_2$ . Therefore, the change of apparent interfacial tension is largely attributed to the relaxation process related to  $\lambda_1$ . It is known that liquid crystalline polymer molecules are stiff and prone to orientational distortions and the formation of a polydomain structure. We identify  $\lambda_1$  with the deformation and perhaps reorientation of domains, and call it the domain-relaxation time.

These domains are highly stretched and may be even broken up into smaller portions during the spinning of the TLCP fiber. The morphologies of these deformed domains are frozen until the beginning of the retraction of the drop, which suggests that the relaxation of the TLCP drop and the stretched domains occur simultaneously, and the two processes will influence each other. Because the domain-relaxation time  $\lambda_1$  is shorter than the retraction time of the TLCP drop, we expect a rapid initial change of the apparent interfacial tension at the timescale of  $\lambda_1$ . This is clearly borne out by the results of all the models in Figure 5. For  $\lambda_2 > 10^3$  s, the effect of the relaxation of the stretched domains inside the TLCP drop on the apparent interfacial tension becomes much weaker. This corresponds to the apparent interfacial tension declining slowly toward an equilibrium value. The details of the coupling between the macroscopic drop dynamics and the mesoscopic domain relaxation within the TLCP drop remains unclear, although we expect director anchoring on the drop surface to play a central role. This will be the focus of future investigations.

## CONCLUSIONS

The dynamic interfacial properties between the TLCP and the flexible polymer were investigated by measuring the apparent interfacial tension. Four models describing the shape evolution of ellipsoidal drops (the Maffettone–Minale, Marrucci–Santo, Yu–Bousmina, and Jackson–Tucker models) were used to determine the interfacial tension. The results of the four models are fairly consistent, especially toward the later stage of retraction. The apparent interfacial tension decreases in time while the TLCP drop retracts. The change of the apparent interfacial tension is related to the relaxation of stretched domains inside the TLCP drop.

This work was supported by research grants from the National Natural Science Foundation of China (Grants 20174024, 20204007 and 50290090) and the U.S. National Science Foundation (Grants CTS-9984402 and CTS-0229298).

## References

1. Rallison, J. M. *Annu Rev Fluid Mech* 1984, 16, 45.
2. Tucker, C. L.; Moldenaers, P. *Annu Rev Fluid Mech* 2002, 34, 177.
3. Yu, W.; Bousmina, M.; Grmela, M.; Palierne, J. F.; Zhou, C. X. *J Rheol* 2002, 46, 1381.
4. Lee, H. S.; Denn, M. M. *J Rheol* 1999, 43, 1583.
5. Tretheway, D. C.; Leal, L. G. *J Non-Newtonian Fluid Mech* 2001, 99, 81.
6. Hooper, R. W.; De Almeida, V. F.; Macosko, C. W.; Derby, J. J. *J Non-Newtonian Fluid Mech* 2001, 98, 141.
7. Li, X. F.; Denn, M. M. *Phys Rev Lett* 2001, 86, 656.
8. Xing, P.; Bousmina, M.; Rodigue, D.; Kamal, M. R. *Macromolecules* 2000, 33, 8020.
9. Tjahjadi, M.; Ottino, J. M.; Stone, H. A. *AIChE J* 1994, 40, 385.
10. Graebbling, D.; Muller, R. *Colloid Surf* 1991, 55, 89.
11. Taylor, G. I. *Proc R Soc A* 1934, 146, 501.
12. Carriere, C. J.; Cohen, A.; Arends, C. B. *J Rheol* 1989, 33, 681.
13. Carriere, C. J.; Cohen, A. *J Rheol* 1991, 35, 205.
14. Luciani, A.; Champagne, M. F.; Utracki, L. A. *J Polym Sci B: Polym Phys* 1997, 35, 1392.
15. Guido, S.; Villone, M. *J Colloid Interface Sci* 1999, 209, 247.
16. Machiels, A. G. C.; Busser, R. J.; Van Dam, J.; Posthuma De Boer, A. *Polym Eng Sci* 1998, 38, 1536.
17. Wu, J.; Mather, P. T. *Proc 74th Annu Meeting Soc Rheol* 2002, 10, HS12.
18. Kim, W. N.; Denn, M. M. *J Rheol* 1992, 36, 1477.
19. Tomokita, S. *Proc R Soc A* 1935, 150, 322.
20. Maffettone, P. L.; Minale, M. *J Non-Newtonian Fluid Mech* 1998, 78, 567.
21. Sigillo, I.; Di Santo, L.; Guido, S.; Grizzuti, N. *Polym Eng Sci* 1997, 37, 1540.
22. Jackson, N. E.; Tucker, C. L. *J Rheol* 2003, 47, 695.
23. Yu, W.; Bousmina, M. *J Rheol* 2003, 47, 1001.
24. Yu, W.; Bousmina, M.; Zhou, C. X. *Rheol Acta* 2004, in press.
25. Mo, H. Y.; Zhou, C. X.; Yu, W. *J Non-Newtonian Fluid Mech* 2000, 91, 221.
26. Wetzel, E. D.; Tucker, C. L. *J Fluid Mech* 2001, 426, 199.
27. Honerkamp, J.; Weese, J. *Continuum Mech Thermodyn* 1990, 2, 17.
28. Colby, R. H.; Nentwich, L. M.; Clingman, S. R.; Ober, C. K. *Europhys Lett* 2001, 54, 269.